ERROR CONTROL FOR PHASE CHANGE PROBLEMS

R.H. NOCHETTO
Department of Mathematics and Institute for Physical Science and Technology, University of Maryland
College Park,MD 20742, USA

A. SCHMIDT
Institut für Angewandte Mathematik, Universität Freiburg
7800 Freiburg, Germany

AND

C. VERDI
Dipartimento di Matematica, Università di Milano
20133 Milano, Italy

1. Introduction

The presence of interfaces, and associated lack of regularity, is responsible for global numerical pollution effects for phase change problems. A cure consists of equidistributing discretization errors in adequate norms by means of highly graded meshes and varying time steps. Their construction relies on *a posteriori* error estimates, which are a fundamental component for the design of reliable and efficient adaptive algorithms for PDEs. These issues have been recently tackled in [6], [7], [8], and are briefly discussed here.

We consider for simplicity the classical two-phase Stefan problem

$$\partial_t u - \Delta\beta(u) = f \quad \text{in } Q = \Omega \times (0,T), \tag{1}$$

where $\beta(s) = \min(s,0) + \max(s-1,0)$; this corresponds to an ideal material with constant thermal properties and unit latent heat. A discrete solution U of (1) satisfies

$$\partial_t U - \Delta\beta(U) = f - \mathcal{R} \quad \text{in } Q, \tag{2}$$

where $\mathcal{R}$, a distribution with singular components and oscillatory behavior, is the so-called *parabolic residual*. Its size is to be determined in negative norms which entail averaging and thus quantify oscillations better.

In §2 we show how to represent the error $e_{\beta(u)} = \beta(u) - \beta(U)$ in terms of $\mathcal{R}$, and in §3 we state an error estimate of the form

$$\|e_{\beta(u)}\|_{L^2(Q)} \leq \mathcal{E}(U, f, T, \Omega; h, \tau),$$

with computable right hand side; hereafter h stands for the meshsize and τ for the time step. This formula is the basis of the adaptive algorithm of §4 and the simulations of §5. We finally show in §6 that $\mathcal{E}(U, f, T, \Omega; h, \tau) \to 0$ as $h, \tau \to 0$, and thereby that the algorithm converges.

2. Error Representation Formula

Upon subtracting (2) from (1) and integrating by parts against a smooth test function φ, the error $e_u = u - U$ satisfies the equation

$$\int_\Omega e_u(T)\varphi(T) = \int_\Omega e_u(0)\varphi(0) + \int_Q e_u(\partial_t\varphi + b\Delta\varphi) + \mathcal{R}(\varphi), \qquad (3)$$

where $b(x,t) = \dfrac{\beta(u) - \beta(U)}{u - U}$ provided $u \neq U$ and $b(x,t) = 1$ otherwise, and

$$\mathcal{R}(\varphi) = \int_\Omega U(0)\varphi(0) - \int_\Omega U(T)\varphi(T) + \int_Q (f\varphi + U\partial_t\varphi + \beta(U)\Delta\varphi). \qquad (4)$$

This motivates the study of the backward parabolic problem in *nondivergence* form [4], with vanishing diffusion coefficient $0 \leq b \leq 1$,

$$\partial_t\psi + (b + \delta)\Delta\psi = -b\chi \quad \text{in } Q, \qquad \psi(T) = 0 \quad \text{in } \Omega, \qquad (5)$$

where $\chi \in L^2(Q)$ and $\delta \downarrow 0$. The theory of nonlinear strictly parabolic problems [3] yields existence of a unique solution ψ, which satisfies [6]

$$\|\nabla\psi(t)\|_{L^2(\Omega)},\ \tfrac{1}{2}\|\partial_t\psi\|_{L^2(Q)},\ \delta^{1/2}\|\Delta\psi\|_{L^2(Q)} \leq \|\chi\|_{L^2(Q)}. \qquad (6)$$

Equation (5) does not exhibit a regularizing effect in that $\|\Delta\psi\|_{L^2(Q)}$ is never bounded uniformly in δ; compare with [2]. Using (6), together with $be_u = e_{\beta(u)}$ and $|e_u| \leq 1 + |e_{\beta(u)}|$, (3) with $\varphi = \psi$ yields

$$(1 - \delta^{1/2})\|e_{\beta(u)}\|_{L^2(Q)} \leq \|e_u(0)\|_{H^{-1}(\Omega)} + \sup_{\substack{\chi \in L^2(Q) \\ 0 < t < T}} \frac{|\mathcal{R}(\psi)|}{\|\nabla\psi(t)\|_{L^2(\Omega)}} + |Q|^{1/2}\delta^{1/2}.$$

Taking $\delta \downarrow 0$ we deduce a representation formula based on evaluating $\mathcal{R}$ in the negative norm $L^1_t H^{-1}_x$, and valid for *any* numerical method:

$$\|e_{\beta(u)}\|_{L^2(Q)} \leq \|e_u(0)\|_{H^{-1}(\Omega)} + \sup_{\substack{\chi \in L^2(Q) \\ 0 < t < T}} \frac{|\mathcal{R}(\psi)|}{\|\nabla\psi(t)\|_{L^2(\Omega)}}.$$

3. A Posteriori Error Estimators

We denote by τ_n the time step at the n-th step and set $t^n = \sum_{i=1}^n \tau_i$. Let $\mathcal{M}^n$ be a uniformly regular partition of Ω into simplices, with meshsize density h_n, and $\mathcal{B}^n$ be the collection of interior sides e of $\mathcal{M}^n$ in Ω; h_S (h_e) stands for the size of $S \in \mathcal{M}^n$ ($e \in \mathcal{B}^n$). Let $\mathbf{V}^n \subset H_0^1(\Omega)$ be the piecewise linear finite element space over $\mathcal{M}^n$ and I^n the Lagrange interpolation operator.

The discrete problem reads as follows. The discrete initial enthalpy $U^0 \in \mathbf{V}^0$ is an "interpolant" of u_0. Given $U^{n-1}, \Theta^{n-1} \in \mathbf{V}^{n-1}$, then $\mathcal{M}^{n-1}$ and τ_{n-1} are modified as described below to get $\mathcal{M}^n$ and τ_n and thereafter $U^n, \Theta^n \in \mathbf{V}^n$ computed according to $\Theta^n = I^n\beta(U^n)$ and

$$\frac{1}{\tau_n}\int_\Omega I^n((U^n - U^{n-1})\varphi) + \int_\Omega \nabla\Theta^n \cdot \nabla\varphi = \int_\Omega I^n(f(t^n)\varphi) \quad \forall\ \varphi \in \mathbf{V}^n. \tag{7}$$

Using mass lumping and enforcing $\Theta^n = I^n\beta(U^n)$ solely at the nodes introduces some consistency errors but amounts to having a monotone problem easy to implement and solved via an optimized nonlinear SOR [5].

If we set $U_t^n = (U^n - I^nU^{n-1})/\tau_n$ and $R^n = I^nf(t^n) - U_t^n$, integrate (4) by parts, and use Galerkin orthogonality (7), we easily arrive at

$$\begin{aligned}\mathcal{R}(\psi) = \mathcal{C} + \sum_n \int_{t^{n-1}}^{t^n}\int_\Omega \Big(R^n(\psi - \Psi) - \nabla\Theta^n \cdot \nabla(\psi - \Psi)\Big) \\ + \sum_n \int_\Omega (U^{n-1} - I^nU^{n-1})\psi^{n-1} + \sum_{n=1}^N \int_{t^{n-1}}^{t^n}\int_\Omega U_t^n(\psi - \psi^{n-1}),\end{aligned}$$

where Ψ is any discrete approximation of ψ and $\mathcal{C}$ stands for consistency terms. Integrating $\nabla\Theta^n$ by parts elementwise and using (6), we conclude

$$\mathcal{E}(U, f, T, \Omega; h, \tau) = C(\mathcal{E}_0 + \mathcal{E}_1 + \mathcal{E}_2 + \mathcal{E}_3 + \mathcal{E}_4) + \mathcal{E}_\mathcal{C}.$$

Here C depends on the minimum angle of $\mathcal{M}^n$, the error indicators $\mathcal{E}_i$ are

$$\begin{aligned}
\mathcal{E}_0 &= \|u_0 - U^0\|_{H^{-1}(\Omega)} && \text{initial error,}\\
\mathcal{E}_1 &= \sum_n \tau_n\Big(\sum_{e\in\mathcal{B}^n} h_e\|[\![\nabla\Theta^n]\!]_e \cdot \nu_e\|_{L^2(e)}^2\Big)^{1/2} && \text{jump residual,}\\
\mathcal{E}_2 &= \sum_n \tau_n\Big(\sum_{S\in\mathcal{M}^n} h_S^2\|R^n\|_{L^2(S)}^2\Big)^{1/2} && \text{interior residual,}\\
\mathcal{E}_3 &= \sum_n \|I^nU^{n-1} - U^{n-1}\|_{H^{-1}(\Omega)} && \text{coarsening,}\\
\mathcal{E}_4 &= \Big(\sum_n \tau_n\|U^n - I^nU^{n-1}\|_{L^2(\Omega)}^2\Big)^{1/2} && \text{time residual,}
\end{aligned}$$

and $\mathcal{E}_\mathcal{C}$ stands for consistency errors which we do not specify and could in principle be removed at the expense of complicating the implementation of (7); see [6]. All indicators $\mathcal{E}_i$ can be evaluated in terms of the computed solution, initial datum, and source term, and are essential; they are also present for the heat equation [2]. The weights of $\mathcal{E}_1, \mathcal{E}_2$ correspond to H^1_x regularity of ψ, as opposed to H^2_x regularity for the heat equation, thereby reflecting the degenerate nature of (1). An alternative approach exploiting the additional, but nonuniform, regularity $\delta\|\Delta\psi\|_{L^2(Q)} \leq \|\chi\|_{L^2(Q)}$ is proposed in [6] and improves on this distinctive aspect of (1).

4. Adaptive Algorithm

The error estimators of §3 entail an L^1 or L^2 norm in time, which is impractical in that the entire history would be needed to control $\mathcal{E}(U, f, T, \Omega; h, \tau)$. We therefore resort to an L^∞ norm in time, and the ensuing equidistribution strategy of minimizing the spatial degrees of freedom for a uniform error distribution in time. For each $S \in \mathcal{M}^n$, the resulting *local* spatial error indicators are denoted by $E_0(S)$, for initial error, and

$$
\begin{aligned}
E_1(S) &= \tfrac{1}{2} T^2\, h_S\, \|[\![\nabla\Theta^n]\!]_e \cdot \nu_e\|^2_{L^2(\partial S)} && \text{local jump residual,}\\
E_2(S) &= T^2\, h_S^2\, \|R^n\|^2_{L^2(S)} && \text{local interior residual,}\\
E_3(S) &= T^2\, \tau_n^{-2}\, \|I^n U^{n-1} - U^{n-1}\|^2_{L^2(S))} && \text{local coarsening.}
\end{aligned}
$$

Let ε be a given error tolerance and $M^n = \operatorname{card} \mathcal{M}^n$. The objective is to select adaptively time steps and mesh densities in such a way that $E_i(S)$ have comparable size for all $S \in \mathcal{M}^n$ (equidistribution) and $\mathcal{E}(U, f, T, \Omega; h, \tau) \leq \varepsilon$. Elements S are either refined or coarsened via *bisection*. This algorithm creates *compatible* consecutive meshes, extends naturally from 2D to 3D, and is handy for combined refinement/coarsening operations [1].

Given refinement and coarsening parameters satisfying $\Gamma_0 + \Gamma_\tau + \Gamma_h \leq 1$, $\gamma_\tau < \Gamma_\tau$, $\gamma_h < \Gamma_h$, the initial mesh is obtained upon bisecting a coarse partition $\mathcal{M}^0$ until $E_0(S) \leq \Gamma_0^2 \varepsilon^2 / M^0$ for all $S \in \mathcal{M}^0$. Neglecting all terms $\mathcal{E}_\mathcal{C}$ for simplicity, the meshsize and time step are modified as follows. We first check whether

$$
\frac{\gamma_h^2}{M^n}\, \varepsilon^2 < \max(E_1(S), E_2(S), E_3(S)) < \frac{\Gamma_h^2}{M^n}\, \varepsilon^2 \quad \forall\, S \in \mathcal{M}^n,
$$

or not. If the rightmost constraint is violated, then S is bisected, whereas the leftmost constraint is used to flag S for coarsening. The latter will be allowed only if the local error incurred is sufficiently small; this is a critical computational issue. We next verify whether

$$
\gamma_\tau\, \varepsilon < T^{1/2} \|U^n - I^n U^{n-1}\|_{L^2(\Omega)} < \Gamma_\tau\, \varepsilon,
$$

or not. Failure of the rightmost inequality forces τ_n to diminish, whereas that of the leftmost constraint causes a corresponding increase of next time step τ_{n+1} but acceptance of the current time step.

5. Numerical Experiments

Our approach is able to detect the presence of interfaces, and refine accordingly, and is insensitive to topological changes such as merging, extinction, and mush or singularity formation. The interface velocity need not be computed explicitly for mesh design, which is a major improvement with respect to [5]. Further simulations, comparisons with several other nonlinear solvers, and a detailed description of the adaptive algorithm (hierarchical data structures, mesh modification strategy, etc.) are examined in [8].

5.1. EXAMPLE 1: OSCILLATING CIRCLE

The interface is a circle of center $c(t)$ moving with velocity $V(t) = \dot{c}(t)$ and changing radius $R(t)$. The exact solution is given by

$$u(x,t) = \begin{cases} \alpha(r^2 - R^2) & \text{if } r \le R \\ 1 + (2\alpha R - V \cdot \frac{x-c}{r} - \dot{R})(r - R) & \text{if } r > R, \end{cases}$$

where $r = |x - c|$ and $\alpha > 0$ is a constant, such that $u > 1$ when $r > R$. The numerical simulation was done in $\Omega = (-1,1)^2$ for $t \in (0,1)$ with

$$c(t) = (0.25,\, 0.4\,\sin(10\,t)), \quad R(t) = 0.35 + 0.2\,\sin(20\,t), \quad \alpha = 17.0\,.$$

Numerical parameters for the adaptive method were

$$\varepsilon = 175,\ \Gamma_0 = 0.1,\ \Gamma_\tau = 0.2,\ \Gamma_h = 0.6,\ \gamma_\tau = 0.155,\ \gamma_h = 0.268\,.$$

Figures 1 and 2 show discrete isothermal lines and corresponding meshes. The innermost isothermal $\Theta = 0$ is the free boundary. Values (and derivatives) of the solution, along with normal interface velocities, exhibit a large variation in time, depending on R and V. This explains the various levels of mesh refinement and the variation in time of the element count.

5.2. EXAMPLE 2: OSCILLATING SOURCE

This is a phase change in a container $\Omega = (-1,1)^2$, $T = 20.0$, with initial temperature $\Theta(x,0) = 0.1\,x_2$, prescribed temperature at three walls $\Theta(x,t) = 0.1\,x_2$ for $x_2 > -1$, a fourth insulated wall $\partial_\nu\Theta(x,t) = 0$ for $x_2 = -1$, and two circular oscillating heat sources driving the evolution,

$$\begin{aligned} f(x,t) = \cos(0.2\,t)\, &\max\left(0.0,\, 3.125 - 50|x - (-0.2,-0.5)|^2\right) \\ &+ \sin(0.2\,t)\max\left(0.0,\, 3.125 - 50|x - (-0.2,0.5)|^2\right). \end{aligned}$$

The exact solution is unknown. The upper pictures of Figure 3 show a topology change consisting of two liquid phases merging. The lower pictures

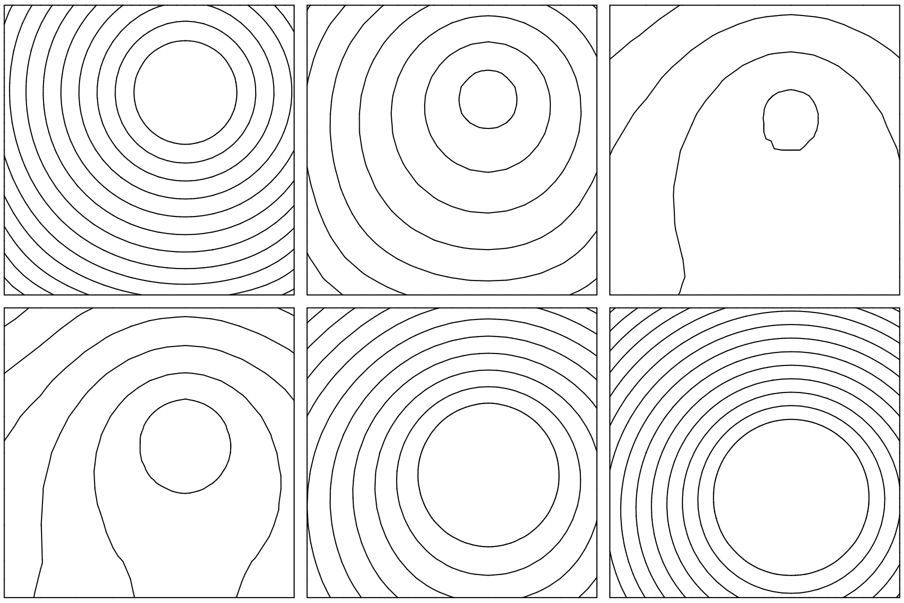

Figure 1. Example 1: Isothermal lines $\Theta = 0, 2, 4, 6, \ldots$ at $t = 0.15, 0.20, 0.25, 0.30, 0.35, 0.40$

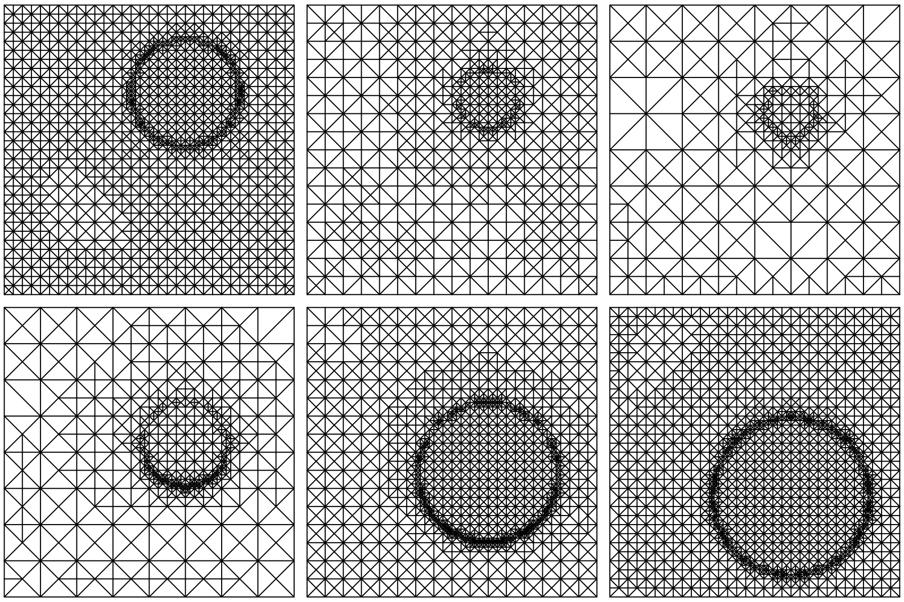

Figure 2. Example 1: Meshes at $t = 0.15, 0.20, 0.25, 0.30, 0.35, 0.40$; element count between 450 and 3600

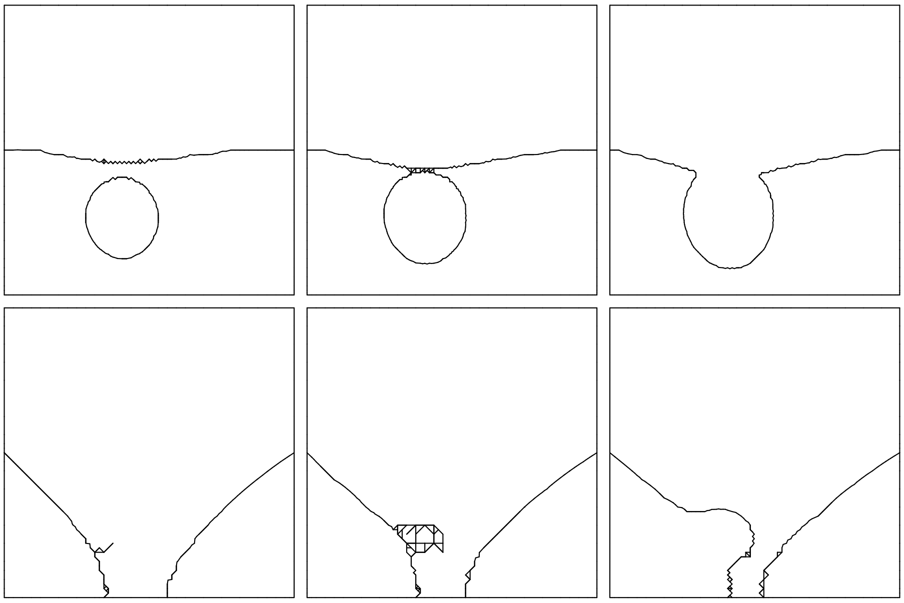

Figure 3. Example 2: Interfaces with topology changes and a mushy region at $t = 1.2, 1.6, 2.0, 8.6, 9.6, 10.6$

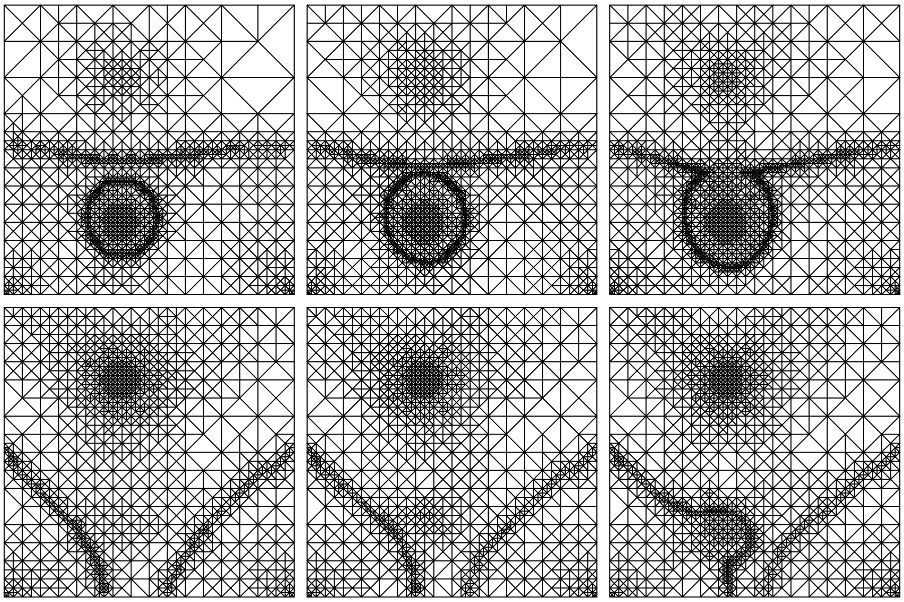

Figure 4. Example 2: Meshes at $t = 1.2, 1.6, 2.0, 8.6, 9.6, 10.6$

show a mushy region produced by a cooling source term. Figure 4 depicts the corresponding meshes with highly refined regions; they capture the interface location along with the presence of strong heat sources.

6. Convergence

It is not obvious that $\mathcal{E}(U, f, T, \Omega; h, \tau) \to 0$ as $h, \tau \to 0$ because $\mathcal{E}$ depends on discrete quantities that change with h and τ. To guarantee convergence further coarsening restrictions are enforced [7]. Assume that

$$\int_\Omega (I^n(U^{n-1})^2 - I^{n-1}(U^{n-1})^2) \leq \tau_{n-1} \int_\Omega |\nabla \Theta^{n-1}|^2,$$

which accounts for the increase in time of L^2_x energy due to mass lumping; this condition is empty with exact integration. Then (7) is *weakly* stable:

$$\max_n \|U^n\|^2_{L^2(\Omega)} + \sum_n \|U^n - I^n U^{n-1}\|^2_{L^2(\Omega)} + \sum_n \tau_n \|\nabla \Theta^n\|^2_{L^2(\Omega)} \leq C. \quad (8)$$

If the additional, and rather restrictive, coarsening constraint is imposed

$$\|U^{n-1} - I^n U^{n-1}\|_{H^{-1}(\Omega)} \leq C\tau_{n-1} \|h_{n-1} \nabla \Theta^{n-1}\|_{L^2(\Omega)}, \quad (9)$$

then the following error estimate results from (8) ($H_n = \max_\Omega h_n$)

$$\|e_{\beta(u)}\|_{L^2(Q)} \leq CT \max_n \left(\tau_n + H_n + \tfrac{H_n^2}{\tau_n}\right).$$

This proves that if $H_n = o(\sqrt{\tau_n})$, which allows for highly graded meshes, the adaptive method converges. Condition (9) measures coarsening in H^{-1}_x, in which I^n does not exhibit superconvergence properties.

References

1. Bänsch, E. (1991) Local mesh refinement in 2 and 3 dimensions, *IMPACT Comput. Sci. Engrg.*, **3**, pp. 181–191
2. Eriksson, K. and Johnson C. (1995) Adaptive finite element methods for parabolic problems IV: nonlinear problems, *SIAM J. Numer. Anal.*, **32**, pp. 1750–1763
3. Ladyzenskaja, O.A., Solonnikov, V. and Ural'ceva, N.N (1968) *Linear and Quasi-linear Equations of Parabolic Type*. AMS, Providence, TMM 23.
4. Nochetto, R.H. (1987) Error estimates for multidimensional singular parabolic problems, *Japan J. Indust. Appl. Math.*, **4**, pp. 111–138
5. Nochetto, R.H., Paolini, M. and Verdi, C. (1991) An adaptive finite elements method for two-phase Stefan problems in two space dimensions. Part II: implementation and numerical experiments, *SIAM J. Sci. Statist. Comput.*, **12**, pp. 1207–1244
6. Nochetto, R.H., Schmidt, A. and Verdi, C. (1997) A posteriori error estimation and adaptivity for degenerate parabolic problems, submitted
7. Nochetto, R.H., Schmidt, A. and Verdi, C. (1997) Mesh and time step modification for degenerate parabolic problems, in preparation
8. Nochetto, R.H., Schmidt, A. and Verdi, C. (1997) Adaptive algorithm and simulations for Stefan problems in two and three dimensions, in preparation